

Evaluation of scalar structure-specific ground motion intensity measures for seismic response prediction of earthquake resistant 3D buildings

Konstantinos G. Kostinakis* and Asimina M. Athanatopoulou^a

*Department of Civil Engineering, Aristotle University of Thessaloniki
Aristotle University Campus, 54124, Thessaloniki, Greece*

(Received February 2, 2015, Revised May 26, 2015, Accepted June 15, 2015)

Abstract. The adequacy of a number of advanced earthquake Intensity Measures (IMs) to predict the structural damage of earthquake resistant 3D R/C buildings is investigated in the present paper. To achieve this purpose three symmetric in plan and three asymmetric 5-storey R/C buildings are analyzed by nonlinear time history analysis using 74 bidirectional earthquake records. The two horizontal accelerograms of each ground motion are applied along the structural axes of the buildings and the structural damage is expressed in terms of the maximum and average interstorey drift as well as the overall structural damage index. For each individual pair of accelerograms the values of the aforementioned seismic damage measures are determined. Then, they are correlated with several strong motion scalar IMs that take into account both earthquake and structural characteristics. The research identified certain IMs which exhibit strong correlation with the seismic damage measures of the studied buildings. However, the degree of correlation between IMs and the seismic damage depends on the damage measure adopted. Furthermore, it is confirmed that the widely used spectral acceleration at the fundamental period of the structure is a relatively good IM for medium rise R/C buildings that possess small structural eccentricity.

Keywords: structure-specific intensity measures; seismic response; nonlinear time history analysis; scalar ground motion IMs; bidirectional excitation; R/C buildings

1. Introduction

During the process of the Performance-Based Earthquake Engineering (PBEE) (Cornell and Krawinkler 2000) the expected damage caused by earthquakes of different intensities must be estimated. The uncertainties associated with this estimation strongly depend on the choice of the parameter describing the intensity of the strong motion. The efficiency of such a parameter can be evaluated with the aid of the correlation degree between the chosen seismic Intensity Measure (IM) and an Engineering Demand Parameter (EDP) accounting for the structural performance. The advantages of an efficient IM are that it improves the accuracy of the assessment of the seismic

*Corresponding author, Ph.D., E-mail: kkostina@civil.auth.gr

^aProfessor, E-mail: minak@civil.auth.gr

response and, as a consequence, it requires a smaller number of nonlinear time history analyses to achieve a desired level of confidence in the context of PBEE. In particular, efficiency means that the variation in the estimated demand for a given IM value is small. Consequently, the identification of an optimal IM, which sufficiently correlates with the seismic damage, is of great importance.

The expected seismic performance is expressed in terms of a chosen EDP. This is usually based on displacement demands, such as maximum and average interstorey drift, as well as deformation demands in the structural elements (rotation/curvature ductility demands). On the other hand, several simple-to-elaborate conventional IMs that can be generated directly from the recorded ground-motion time-history have been used to estimate the damage potential of ground motions (e.g., Elenas and Meskouris 2001, Yakut and Yilmaz 2008, Masi *et al.* 2011, Cantagallo *et al.* 2012). Moreover, alternative advanced scalar IMs have been proposed. These IMs are structure-specific, that is they take into account not only ground motion characteristics but also structural information (e.g., modal vibration properties or even data from pushover curve) in order to reduce the scatter of the selected damage response parameter. The benefit is that the number of records required to be used in the process of PBEE can be significantly reduced (Benjamin and Cornell 1970).

Many researchers proposed scalar structure-specific IMs and they investigated their ability to predict the structural performance (e.g., Cordova *et al.* 2000, Luco and Cornell 2007, Mehanny 2009, Kadas *et al.* 2011). They found that the structure specific IMs can adequately predict the seismic response of planar moment-resisting frames. Fontara *et al.* (2012) examined the correlation between a number of advanced, structure-specific ground motion IMs and the structural damage of multistorey R/C regular and irregular planar frames. It was shown that the IMs which account for the period elongation due to nonlinear response indicate the strongest correlation with the structural damage for low as well as high nonlinear response.

It must be noted that, as mentioned before, all the above investigations were restricted to planar R/C frames, thus accounting for only one component of the strong motion records. Modern seismic codes (ASCE/SEI 41-06, EC8, FEMA 356, NEHRP, UBC) suggest that structures shall be designed for the two horizontal translational components of ground motion (in the majority of buildings the vertical component can be neglected). In a preliminary study, Kostinakis *et al.* (2014) investigated the adequacy of eight structure-specific IMs as predictors of the seismic damage in case of 3D R/C buildings. They analyzed two 5-storey R/C buildings, a symmetric and an asymmetric one, for 20 bidirectional ground motions. The structural performance was expressed in terms of maximum interstorey drift as well as the overall structural damage index.

The objective of the present paper is to investigate the correlation between ten advanced, scalar structure-specific ground motion IMs and the structural response of earthquake resistant 3D R/C buildings under bidirectional excitation. For this purpose six medium-rise R/C buildings are studied. All buildings have five stories and their structural systems consist of vertical elements in two perpendicular directions (axes x and y). The buildings, which have been designed on the basis of EC8 and EC2 provisions, are analyzed by means of Nonlinear Time History Analysis (NTHA) for 74 bidirectional strong motions. For the evaluation of the expected structural damage state of each building the Park and Ang overall structural damage index (Park and Ang 1985), as well as the maximum and average interstorey drift are used as damage measures. The results show that the interdependency between the IMs and the expected seismic damage depends on the special structural characteristics and on the damage measure adopted. Moreover, it is verified that the widely used spectral acceleration at the fundamental period of the structure is a relatively good

indicator of the structural damage for medium-rise R/C buildings with small eccentricity.

2. Steps of the followed procedure

The procedure followed in order to achieve the goals of the present investigation consists of the following steps:

- (a) Selection of the examined R/C buildings
- (b) Modeling of the elastic and inertia behavior
- (c) Design of the structural members
- (d) Modeling of the nonlinear behavior of the buildings
- (e) Selection of the ground motions used for the nonlinear analyses
- (f) Nonlinear time history analysis of the buildings
- (g) Computation of damage indicators for the structural members and estimation of the damage state of each building as a whole, using three different EDPs
- (h) Choice of a number of scalar structure-specific IMs and their determination for each bidirectional earthquake record
- (i) Assessment of the examined IMs as predictors of the seismic damage for the six buildings under investigation

In the following paragraphs, the details of the aforementioned steps are presented.

3. Description of the individual steps

3.1 Selection of the buildings (step a)

For the purposes of the present investigation, three double-symmetric and three asymmetric in plan R/C buildings, with data supplied in Figs. 1 and 2 are studied. All buildings have five stories and a structural system that consists of members in two perpendicular directions (axes x and y). More specifically, the following buildings are investigated (the classification follows the classification of structural types reported in EC8):

- Symmetric Frame System along both axes x and y SFxy: Double-symmetric building without walls (Fig. 1a).
- Symmetric Wall System along both axes x and y SWxy: Double-symmetric building with walls that take 80% of the base shear along both axes x and y (Fig. 1b).
- Symmetric Wall System along axis x and Frame System along axis y SWxFy: Double-symmetric building with walls that take more than 70% of the base shear along axis x , and without walls along axis y (Fig. 1c).
- Asymmetric Frame System along both axes x and y AFxy: Asymmetric in plan building without walls (Fig. 2a).
- Asymmetric Wall System along both axes x and y AWxy: Asymmetric in plan building with walls that take 67% of the base shear along axis x and 70% of the base shear along axis y (Fig. 2b).
- Asymmetric Frame System along axis x and Wall System along axis y AFxWy: Asymmetric in plan building with walls that take 70% of the base shear along axis y , and without walls along axis x (Fig. 2c).

All the above buildings are chosen so as to represent a large amount of R/C buildings designed

with the aid of EC8 in the Mediterranean area. It must be noted that the structural systems of the chosen buildings cover the most usual systems suggested in EC8. All buildings are regular in elevation according to the criteria set by EC8. Moreover, in order to investigate the influence of the structural eccentricity on the results, the choice of the asymmetric buildings was made bearing in mind that their structural systems must correspond to those of the double-symmetric ones. The structural eccentricity e_0 of the asymmetric buildings fulfils one of the following inequalities: $e_{0x} > 0.30r_x$ or $e_{0y} > 0.30r_y$. Therefore, these buildings display a high degree of asymmetry and can be classified as irregular in plan. In Table 1 all the common design data of the examined buildings are presented.

3.2 Elastic modeling (step b)

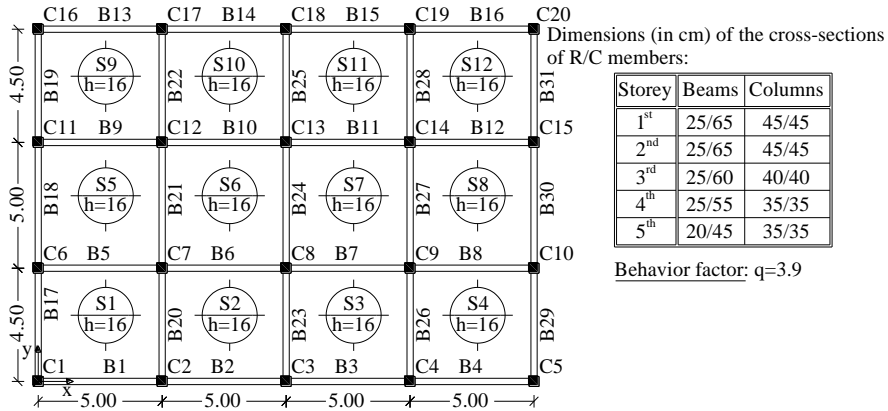
For the buildings' modeling all basic recommendations of EC8, such as the diaphragmatic behavior of the slabs, the rigid zones in the joint regions of beams/columns and beams/walls and the values of flexural and shear stiffness corresponding to cracked R/C elements are taken into consideration. For the modeling of the R/C walls the equivalent frame model is used. All buildings are considered to be fully fixed to the ground. Using the data given in Table 1, the upper limit values of the behavior factor q according to EC8 (§5.2.2.2) were determined for the two principal directions. These are the maximum allowable values of the behavior factor that can be used to design the structural elements of the building. Then the smaller of the two q values was chosen for the two directions. These values are shown in Figs. 1 and 2 and have been used for the design of the examined buildings.

3.3 Design of the structural members (step c)

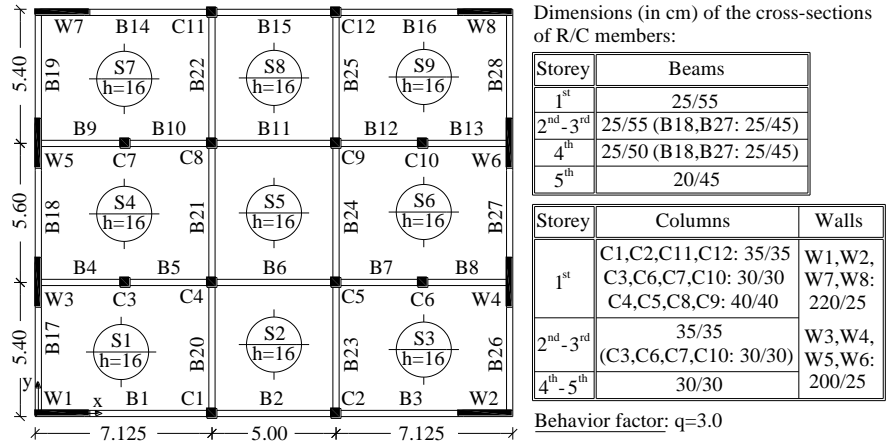
The buildings are analyzed for static vertical loads as well as for earthquake loads. The seismic analysis was performed by using the modal response spectrum method, as defined in EC8, for the design spectrum given in Table 1. The R/C structural elements are designed following the provisions of EC2 and EC8. Consequently, as EC8 states (§5.2.3.3(2)), a capacity design at frame joints is carried out only along the direction, that the buildings belong to the structural type of frame systems or frame-equivalent dual systems. It should also be noted that the choice of the dimensions of the structural members' cross-sections as well as of their reinforcement was made bearing in mind the optimum exploitation of the structural materials strength (steel and concrete). Therefore, the Capacity Ratios CRs (where $CR = \text{Design value of internal force} / \text{Design strength}$) of all the critical cross-sections due to bending and shear are close to 1.0. The professional program for R/C building analysis and design RAF (2012) was employed. The first 6 natural periods as well as the corresponding modal participating mass ratios of all models are given in Table 2.

Table 1 Common design data for all buildings

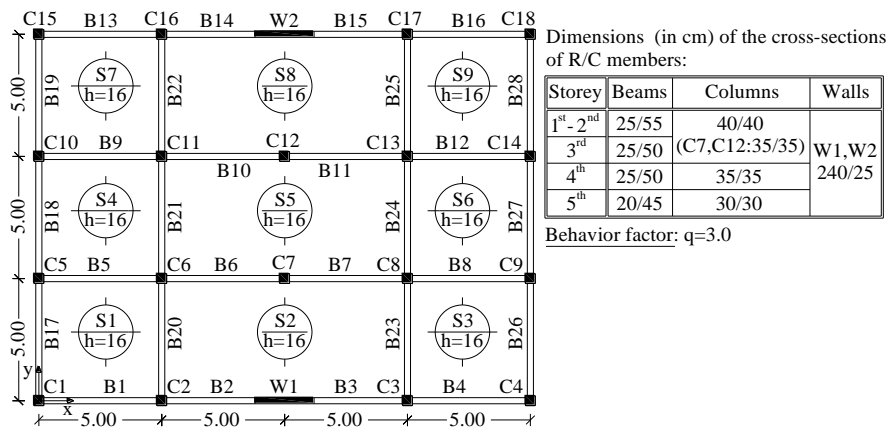
| Stories' heights H_i | Ductility class | Concrete | Steel | Slab loads | Masonry loads | Design spectrum (EC8) |
|------------------------|-----------------|---|--|---|--|---|
| 3.2 m | Medium (DCM) | C20/25 $E_c = 3 \cdot 10^7 \text{ kN/m}^2$ $v = 0.2$ $w = 25 \text{ kN/m}^3$ | S500B $E_s = 2 \cdot 10^8 \text{ kN/m}^2$ $v = 0.3$ $w = 78.5 \text{ kN/m}^3$ | Dead: $G = 5.0 \text{ kN/m}^2$ Live: $Q = 2.0 \text{ kN/m}^2$ | Perimetric beams: 3.6 kN/m^2 Internal beams: 2.1 kN/m^2 | Reference PGA: $a_{gR} = 0.24 \text{ g}$ Importance class: II $\rightarrow \gamma_I = 1$ Ground type: C |



(a)

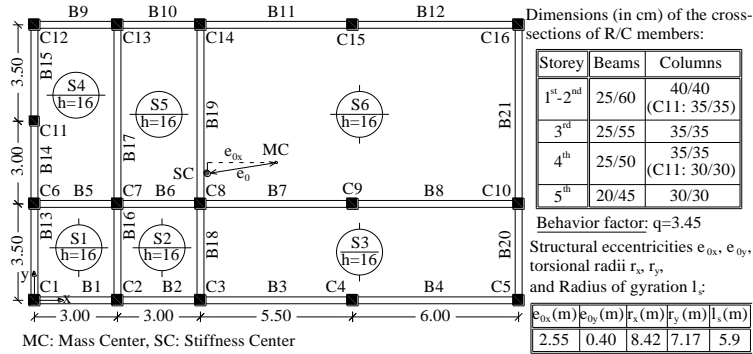


(b)

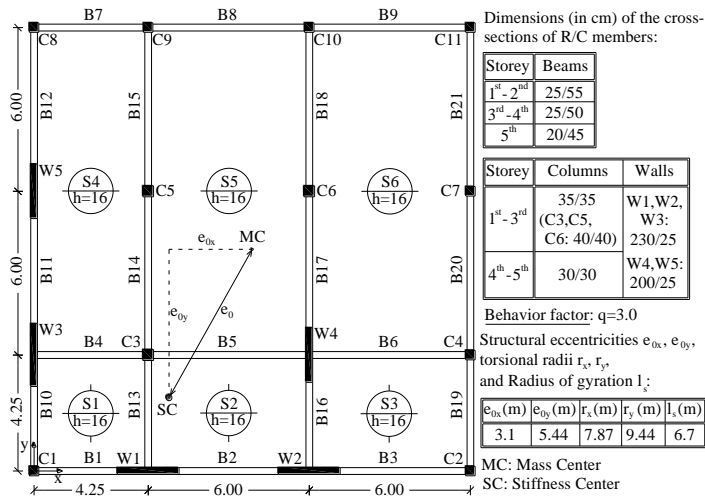


(c)

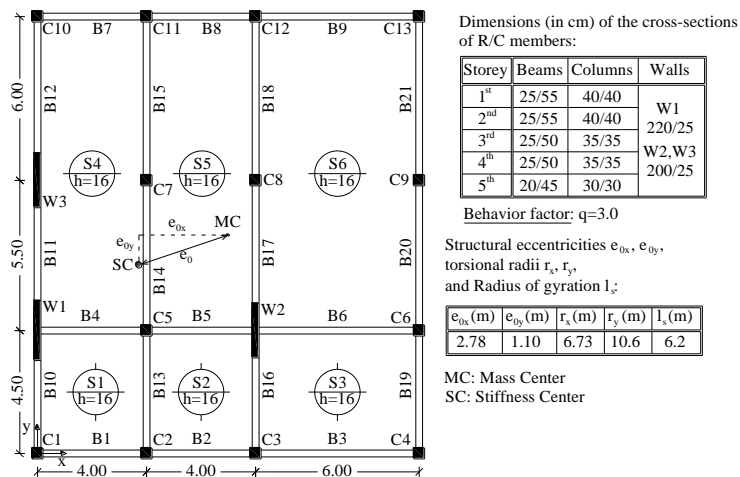
Fig. 1 Plan views and geometrical properties of the double-symmetric buildings (SFxy (a), SWxy (b) and SWxFy (c))



(a)



(b)



(c)

Fig. 2 Plan views and geometrical properties of the asymmetric buildings (AFxy (a), AWxy (b) and AFxWy (c))

3.4 Modeling of the nonlinear behavior (step d)

For the modeling of the buildings' nonlinear behavior lumped plasticity (plastic hinge) models at the column and beam ends as well as at the base of the walls, are used. The Modified Takeda hysteresis model (Otani 1974) (Fig. 3a) is used to model the material inelasticity of the structural members. It is important to notice that the effects of axial load-biaxial bending moments (P-M-M) interaction at column and wall hinges are taken into consideration by means of the P-M-M interaction diagram shown in Fig. 3(b), which is implemented in the software used to conduct the nonlinear time history analyses (Carr 2004). The yield moments as well as the parameters needed to determine the P-M-M interaction diagram of the vertical members' cross sections (Fig. 3b) are determined using appropriate software (Imbsen Software Systems 2006).

Table 2 First 6 natural periods and corresponding modal participating mass ratios

| Mode | SF _{xy} | | | SW _{xy} | | | SW _x F _y | | |
|------|------------------|------------|------------|------------------|------------|------------|--------------------------------|------------|------------|
| | Period T (sec) | x-axis (%) | y-axis (%) | Period T (sec) | x-axis (%) | y-axis (%) | Period T (sec) | x-axis (%) | y-axis (%) |
| 1 | 0.72 | 0 | 77 | 0.69 | 73 | 0 | 1.00 | 0 | 80 |
| 2 | 0.72 | 77 | 0 | 0.65 | 0 | 76 | 0.67 | 75 | 0 |
| 3 | 0.58 | 0 | 0 | 0.42 | 0 | 0 | 0.57 | 0 | 0 |
| 4 | 0.28 | 14 | 0 | 0.19 | 0 | 15 | 0.38 | 0 | 12 |
| 5 | 0.28 | 0 | 14 | 0.19 | 17 | 0 | 0.23 | 0 | 4 |
| 6 | 0.23 | 0 | 0 | 0.11 | 0 | 0 | 0.21 | 16 | 0 |

| Mode | AF _{xy} | | | AW _{xy} | | | AF _x W _y | | |
|------|------------------|------------|------------|------------------|------------|------------|--------------------------------|------------|------------|
| | Period T (sec) | x-axis (%) | y-axis (%) | Period T (sec) | x-axis (%) | y-axis (%) | Period T (sec) | x-axis (%) | y-axis (%) |
| 1 | 0.98 | 1 | 70 | 1.01 | 52 | 11 | 1.03 | 78 | 1 |
| 2 | 0.79 | 78 | 1 | 0.66 | 16 | 59 | 0.74 | 2 | 49 |
| 3 | 0.58 | 1 | 7 | 0.41 | 8 | 6 | 0.46 | 0 | 26 |
| 4 | 0.37 | 0 | 11 | 0.34 | 10 | 2 | 0.37 | 12 | 0 |
| 5 | 0.31 | 12 | 0 | 0.19 | 4 | 12 | 0.25 | 0 | 8 |
| 6 | 0.23 | 0 | 5 | 0.18 | 3 | 1 | 0.23 | 5 | 0 |

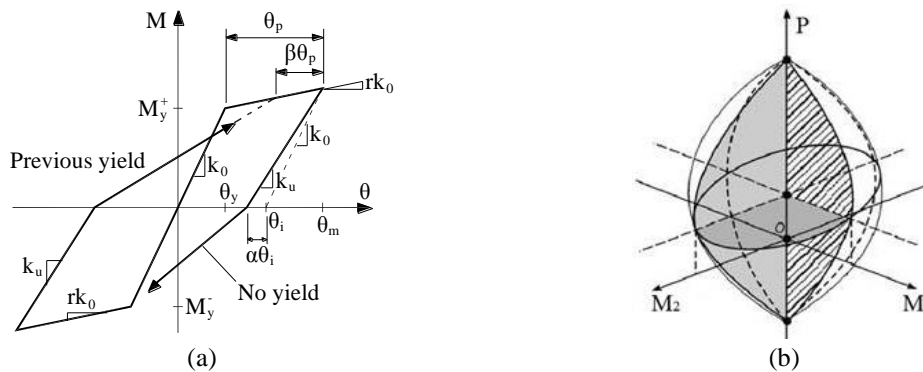


Fig. 3 Moment (M) - Rotation (θ) relationship (a) and P-M₁-M₂ interaction diagram (b) (Carr 2004)

3.5 Earthquake records (step e)

A suite of 74 pairs of horizontal bidirectional earthquake records obtained from the PEER (2003) and the European (2003) strong motion databases are used as input ground motion for the analyses. The seismic records, which have been chosen from worldwide well known sites with strong seismic activity, are recorded on Soil Type C according to EC8 and have magnitudes (M_s) between 5.5 and 7.8. The ground motion set employed is intended to cover a variety of conditions regarding tectonic environment, modified Mercalli intensity and closest distance to fault rapture, thus representing a wide range of intensities and frequency content. Another aspect considered on the selection of the seismic records is that they provide a wide spectrum of structural damage, from negligible to severe, to the buildings investigated in the present study.

The recorded horizontal accelerograms of each ground motion are transformed to the corresponding uncorrelated ones rotating them about the vertical axis by the angle θ_o (Eq. (1)) (Penzien and Watabe 1975). Then, the pairs of the uncorrelated accelerograms are used as seismic input for the analyses of the structures, as ASCE 41-06 proposes. The characteristics of the input ground motions are shown in Table A.1 along with the correlation factor of the recorded components ρ (Penzien and Watabe 1975), which is given by Eq. (1)

$$\rho = \frac{\sigma_{xy}}{(\sigma_{xx} \cdot \sigma_{yy})^{1/2}}, \quad \tan 2\theta_o = \frac{2\sigma_{xy}}{\sigma_{xx} - \sigma_{yy}} \quad \text{with} \quad \sigma_{ij} = \frac{1}{t_{tot}} \cdot \left(\int_0^{t_{tot}} \alpha_i(t) \cdot \alpha_j(t) dt \right) \quad i = x, y \quad (1)$$

where $\alpha_x(t)$ and $\alpha_y(t)$ are the recorded ground acceleration histories along two horizontal orthogonal directions; σ_{xx} , σ_{yy} are the quadratic intensities of $\alpha_x(t)$ and $\alpha_y(t)$ respectively; σ_{xy} is the corresponding cross-term; and t_{tot} is the duration of the ground motion.

3.6 Nonlinear time history analyses - Damage indicators (steps f, g)

The six buildings presented in section 3.1 are analyzed by Nonlinear Time History Analysis (NTHA) for each one of the 74 pairs of earthquake records taking into account the design vertical loads of the structures. The analyses are performed with the aid of the computer program Ruaumoko (Carr 2004). The two horizontal uncorrelated accelerograms of each ground motion are applied along the structural axes. For each ground motion the damage state of the six buildings is determined. The damage state is expressed in the form of the following EDPs: i) the Maximum Interstorey Drift Ratio (MIDR), ii) the Average Interstorey Drift Ratio (AIDR) and iii) the Overall Structural Damage Index (OSDI). The aforementioned structural response parameters were chosen, since they lump the existing damage in all the cross-sections in a single value, which can be easily correlated to scalar seismic IMs. So, they have been used by many researchers for the assessment of the inelastic response of structures (e.g., Elenas and Meskouris 2001, Dimova and Negro 2005, Yakut and Yilmaz 2008, Masi *et al.* 2011).

The MIDR, which is generally considered an effective indicator of global structural and nonstructural damage of R/C buildings (e.g., Gunturi and Shah 1992, Naeim 2001) corresponds to the maximum interstorey drift among the storeys' of the four perimeter frames. The AIDR is determined as follows: the horizontal roof displacement of each perimeter frame is computed and then it is divided by the total height of the building. Hence, four values of AIDR are produced. The maximum value among the four ones is considered as damage indicator.

Moreover, the overall structural damage index (OSDI) of the buildings is determined. Note that, in general, damage indices estimate quantitatively the degree of seismic damage that a cross-section as well as a whole structure has suffered. In the present study, the OSDI is computed as a weighted average of the local damage indices at the ends of each structural member. The dissipated energy is used as a weight factor (Eq. (2)) (e.g., Park *et al.* 1987, Elenas and Meskouris 2001, Dimova and Negro 2005)

$$OSDI = \sum_{i=1}^n \left[LDI_i \left(\frac{E_{Ti}}{\sum_{i=1}^n E_{Ti}} \right) \right] \tag{2}$$

where LDI_i is the local damage index at cross section i (Eq. (3)), E_{Ti} is the energy dissipated at the cross section i and n is the number of cross sections at which the local damage is computed. For the LDI, the widely used Park and Ang (1985) damage index modified by Kunnath *et al.* (1992) has been used. The advantages of this damage index are its simplicity and the fact that it has been calibrated against a significant amount of observed seismic damage. It is also important to mention that the Park and Ang damage index was tested experimentally. At a given cross section the local damage index (LDI) is given by Eq. (3)

$$LDI = \frac{\varphi_m - \varphi_y}{\varphi_u - \varphi_y} + \left(\frac{\beta}{M_y \cdot \varphi_u} \right) E_T \tag{3}$$

where φ_m is the maximum curvature observed during the load history, φ_u is the ultimate curvature capacity, φ_y is the yield curvature, E_T is the dissipated hysteretic energy, M_y is the yield moment of the cross section and β is a dimensionless constant determining the contribution of cyclic loading to damage, which is taken equal to 0.5 for the analyses conducted.

In the present study three damage degrees are defined based on the values of OSDI (Park *et al.* 1987): 1) minor for $OSDI < 0.25$, 2) moderate for $0.25 < OSDI < 0.4$ and 3) severe for $OSDI > 0.4$. The number of records which cause minor, moderate and severe damage in the examined buildings are shown in Fig. 4. We should note that no record caused elastic behavior to anyone of the six buildings.

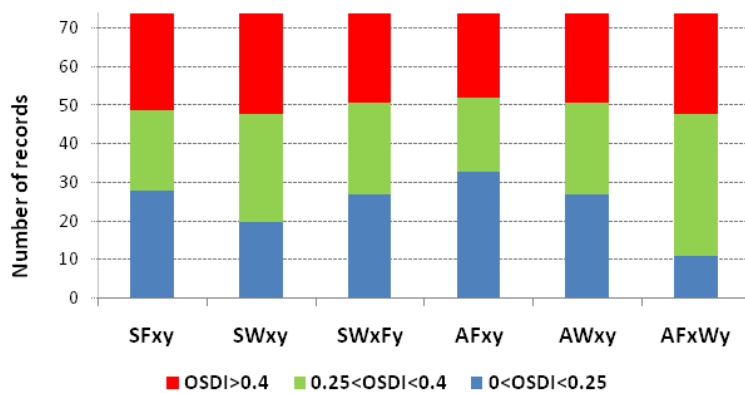


Fig. 4 Number of records corresponding to each damage degree

3.7 Scalar, Structure-specific intensity measures (step h)

The evaluated scalar, structure-specific ground motion IMs are determined via eigenvalue or pushover analyses. It must be noticed that in the cases where a pushover analysis is necessary in order to determine the values of certain IMs, the procedure stated in EC8 for the determination and the bilinearization of the pushover curve is used. The examined IMs were proposed by researchers in an attempt to avoid the major shortcomings associated with $S_a(T_1)$; namely, ignoring both the contribution of higher modes to the overall dynamic response and the increase of the fundamental period of the structure (period elongation) associated with nonlinear behavior. Therefore, all the following IMs are assessed with respect to $S_a(T_1)$ efficiency. More specifically, the following advanced, structure-specific IMs are considered:

- IM proposed by Kappos (1990) (IM_{Kappos})

$$IM_{Kappos} = \int_{T_{1-t}}^{T_{1+t}} S_v(T) dT \quad (4)$$

where S_v is the spectral velocity curve, T_1 the fundamental period of the structure and $t=0.2T_1$.

- IM proposed by Matsumura (1992) ($IM_{Matsumura}$)

$$IM_{Matsumura} = \frac{1}{T_y} \int_{T_y}^{2T_y} S_v(T) dT \quad (5)$$

where T_y is the elastic period of the equivalent SDOF system, which is determined via Pushover Analysis.

- IM proposed by Kadas *et al.* (2011) ($IM_{Kadas \text{ et al.}}$).

$$IM_{Kadas \text{ et al.}} = \frac{1}{(T_f - T_y) a_y} \int_{T_y}^{T_f} S_a(T) (T - T_y) dT \quad (6)$$

where a_y is the yield acceleration, S_a is the spectral acceleration curve and T_f is a softening period, which is determined with the aid of the following relation

$$T_f = 1.07 \cdot T_y \cdot \left[\frac{S_a(T_y)}{a_y} \right]^{0.45} \leq 2.0T_y \quad (7)$$

- IM proposed by Cordova *et al.* (2000) ($IM_{Cordova \text{ et al.}}$)

$$IM_{Cordova \text{ et al.}} = S_a(T_1) \cdot \left[\frac{S_a(2T_1)}{S_a(T_1)} \right]^{0.5} \quad (8)$$

- IM proposed by Mehanny (2009) ($IM_{Mehanny}$)

$$IM_{Mehanny} = S_a(T_1) \cdot \left[\frac{S_a(\sqrt{R} \cdot T_1)}{S_a(T_1)} \right]^{0.5} \quad (9)$$

where $R=V_e/V_y$. V_e is the lateral strength required to maintain the system elastic and V_y is the lateral yielding strength of the equivalent SDOF system which can be determined by Pushover Analysis. It must be noticed that Mehanny introduced the above structure-specific IM in an attempt to improve the adequacy of the $IM_{Cordova \ et \ al.}$. By introducing the multiplier $R^{1/2}$, Mehanny achieved the generalization of the IM described by Eq. (8), since the enhanced IM acquires the ability to self adapt to buildings with different levels of nonlinear response during the strong motion.

- IM proposed by Luco (2002) and Luco and Cornell (2007) ($IM_{Luco \ \& \ Cor}$)

$$IM_{Luco \ \& \ Cor} = \frac{S_d(T_1, d_y)}{S_d(T_1)} \cdot \sqrt{(\Gamma_1 \cdot ID_1 \cdot S_d(T_1))^2 + (\Gamma_2 \cdot ID_2 \cdot S_d(T_2))^2} \quad (10)$$

where Γ_1 and Γ_2 are the 1st and 2nd-mode participation factors respectively (Chopra 2001), ID_1 and ID_2 are the 1st and 2nd-mode interstorey drifts that correspond to the storey at which the quantity under the square root is maximized and $S_d(T_1, d_y)$ is the 1st-mode spectral displacement of an elastic-perfectly-plastic equivalent SDOF with yield displacement d_y .

- IM proposed by Bojorquez and Iervolino (2011) ($IM_{Boj \ \& \ Ier}$).

$$IM_{Boj \ \& \ Ier} = S_a(T_1) \cdot \left[\frac{GMV(S_a(T_1) \dots S_a(2T_1))}{S_a(T_1)} \right]^{0.4} \quad (11)$$

where $GMV(S_a(T_1) \dots S_a(2T_1))$ is the Geometric Mean Value of the spectral acceleration over a range of periods between T_1 and $2T_1$

- IM proposed by Lin (2008) and Lin *et al.* (2011) ($IM_{Lin \ et \ al.}$).

$$IM_{Lin \ et \ al} = S_a(T_1)^{0.5} \cdot S_a(1.5T_1)^{0.5} \quad (12)$$

- IM proposed by Yahyaabadi and Tehranizadeh (2011) for Non-Collapse seismic demand prediction ($IM_{Yah \ \& \ Tehr-NC}$).

$$IM_{Yah \ \& \ Tehr-NC} = \left[0.8S_d^2(T_1) + 0.2S_d^2(1.2T_1) \right]^{0.5} \quad (13)$$

where S_d is the spectral displacement.

- IM proposed by Yahyaabadi and Tehranizadeh (2011) for Collapse seismic demand prediction ($IM_{Yah \ \& \ Tehr-C}$).

$$IM_{Yah \ \& \ Tehr-C} = \left[0.4S_d^2(T_1) + 0.4S_d^2(1.2T_1) + 0.2S_d^2(1.6T_1) \right]^{0.5} \quad (14)$$

where S_d is the spectral displacement.

The aforementioned IMs are determined for each one of the two components of the 74 bidirectional strong motions. However, in order to study the correlation of the IMs with the structural damage of the buildings, it is necessary to represent the intensity parameters corresponding to the two horizontal components by a single value. To achieve this, the Geometric Mean Value (GMV), which is the most widely used expression for the definition of horizontal bidirectional ground motion characteristics (Beyer and Bommer 2006) was used for each seismic excitation

$$IM_{GMV} = \sqrt{IM_1 \cdot IM_2} \quad (15)$$

where IM_1 and IM_2 : values of the IMs determined for each one of the two horizontal components of the ground motion. Three other alternative relations to express the IMs corresponding to the two horizontal components by a single value, that is the arithmetic mean value, the SRSS value and the maximum value over the two values, have been studied in Kostinakis *et al.* (2015). In this study it has been proved that the variant relations to define a single IM corresponding to the two horizontal accelerograms produce the same correlation between IMs and damage measures.

3.8 Assessment of the IMs effectiveness (step i)

As mentioned above, the choice of the appropriate IM is of great significance for the accuracy of the probability-based seismic assessment of a structure. An optimal IM is defined as being efficient, sufficient, practical and robust against scaling (Luco and Cornell 2007, Mehanny 2009). Among the aforementioned desired characteristics of an IM, efficiency is commonly used to establish the superiority of it. The advantages of an efficient IM are that it improves the accuracy of the assessment of the seismic response and, as a consequence, it requires a smaller number of nonlinear time history analyses to achieve a desired level of confidence in the context of PBEE. In particular, efficiency means that the variation in the estimated demand for a given IM value is small. The scatter in structural responses at a given IM due to record-to-record variability provides a relative measure of the efficiency of an IM (Giovenale *et al.* 2004, Mehanny 2009).

There are two different approaches widely used in the literature for the evaluation of the efficiency of a given IM (Giovenale *et al.* 2004). According to the first method the unscaled seismic records are used as input ground motion for the nonlinear dynamic analyses and, as a result, a cloud of data points within the EDP-IM space for the set of the records adopted is received. Then, in order to determine the dispersions of the EDP, a regression analysis is applied to this resulting set of points assuming an adequate functional form for the regression model relating EDP to IM. More specifically, the dispersions of the EDP are evaluated using either the standard deviation (e.g., Mori *et al.* 2004, Luco and Cornell 2007) or an appropriate correlation coefficient (e.g., Elenas and Meskouris 2001, Yakut and Yilmaz 2008, Kadas *et al.* 2011). According to the second approach, the accelerograms are first scaled to multiple levels of intensity, namely to different values of the examined IM (e.g., Cordova *et al.* 2000, Tothong and Luco 2007, Tothong and Cornell 2008, Mehanny 2009). Consequently, nonlinear time history analyses are conducted for each scaled record and the IDA (Incremental Dynamic Analysis) curves for all the seismic motions are determined. A regression analysis is therefore not required and the dispersion of the EDP is directly computed conditioned on each value of the IM.

In the present study, the first approach is used in order to evaluate the efficiency of the examined IMs. In particular, correlation coefficients are determined to express the grade of interdependency between the ground motion IMs and the damage measures of the six buildings. As a first step, the Kolmogorov-Smirnov test is used in order to identify whether the input parameters follow a normal distribution. For the selected set of ground motions, this test showed that, with a 5% error, the examined quantities do not follow the normal distribution. So, for the evaluation of the correlation between the investigated parameters, the Spearman rank correlation coefficient is adopted.

The Spearman's rank correlation coefficient is used as an index to assess how well the relationship between two variables X and Y can be described using a monotonic function. Its value ranges from -1 to 1. The values 1 and -1 indicate that each of the variables is a perfect monotone function of the other, while 0 indicates no association between the ranks of the two variables. The

Spearman rank correlation coefficient between two variables X and Y is given by Eq. (16)

$$P_{\text{Spearman}} = 1 - \frac{6 \sum_{i=1}^N D^2}{N(N^2 - 1)} \quad (16)$$

D : differences between the ranks of corresponding values of X_i and Y_i and

N : number of pairs of values (X, Y) in the data.

4. Comparative assessment of the results

Figs. 5 and 6 illustrate the correlation coefficients after Spearman between the three EDPs (OSDI, MIDR and AIDR) investigated in the present study and the seismic IMs considered for the six buildings.

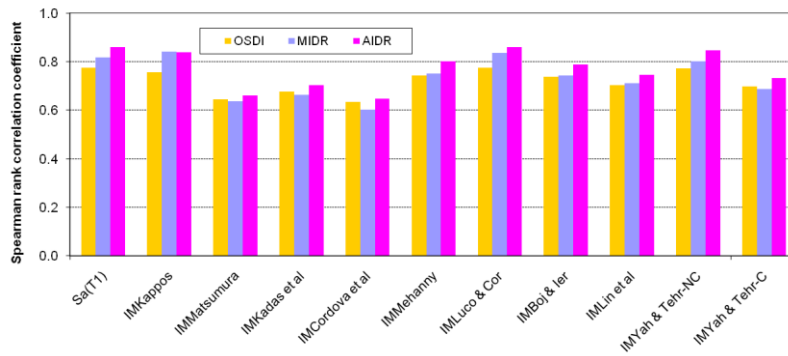
We can see that for the symmetric buildings (Fig. 5) the correlation coefficients between IMs and OSDI attain smaller values than the ones between IMs and MIDR or AIDR. The only exception is the IMs proposed by Kadas *et al.* (2011), by Cordova *et al.* (2000), by Matsumura (1992), as well as by Yahyaabadi and Tehranizadeh for Collapse seismic demand prediction (2011), where the correlation between OSDI and IMs is greater than the correlation between MIDR and IMs in the SFxy model (Fig. 5a). Concerning the two asymmetric models AFxy and AFxWy the same conclusion is valid. That is the correlation is stronger between IMs and MIDR or AIDR than the correlation between IMs and OSDI (Figs. 6a and 6c). However this conclusion is not valid for the AWxy model where the correlation is stronger between IMs and OSDI than the correlation between IMs and MIDR or AIDR (Fig. 6b).

The observation that in the most cases the correlation coefficients between IMs and OSDI attain smaller values than the ones between IMs and MIDR or AIDR can be attributed to the assumptions and the inherent uncertainties of the definition of the OSDI (Eq. (2)). In particular, the analyses showed that, for some ground motions, the damage observed was restricted to a very small number of structural elements, although the rest elements remained elastic. In this case, the value of the OSDI is very large, since the computation of it (Eq. (2)) takes into account only the damaged cross sections and ignores the elastic frame elements, in which the dissipated energy is zero. Such a result is misleading, because in this case large OSDI indicates very significant structural damage of the whole building, whereas, in fact the damage is restricted to few vertical structural elements only.

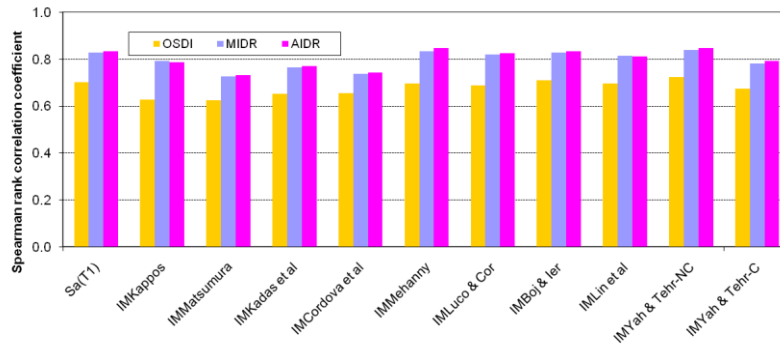
Regarding the other two variables used to express the damage state of the buildings, MIDR and AIDR, the results do not reveal a general trend. See for example that the $IM_{\text{Luco \& Cor}}$ correlates better with MIDR than AIDR for the buildings SWxFy and AFxy (Figs. 5c and 6a). On the contrary, the same IM correlates better with AIDR than MIDR for the buildings SFxy and AWxy (Figs. 5a and 6b), whereas, in case of the structural systems SWxy and AFxWy (Figs. 5b and 6c) these IMs have almost the same grade of correlation.

The IMs that present high correlation with the damage measures (MIDR and AIDR) in the symmetric models are $IM_{\text{Luco \& Cor}}$, $IM_{\text{Yah \& Tehr-NC}}$ and $S_a(T_1)$. The strong correlation between such a simple IM as the $S_a(T_1)$ and the damage measures can be attributed to the fact that the performance of these buildings is dominated by the first two modes of vibration for excitation along x and y

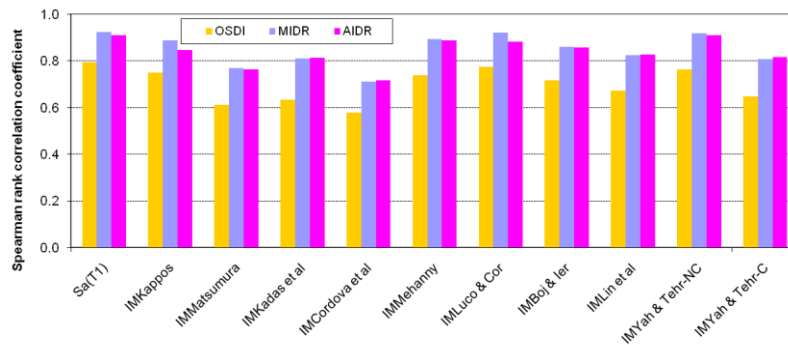
axes. The modal participating mass ratios attain values greater than 70% for at least one of the first two mode shapes. Also we see that in these two modes the translational components of vibration dominate. Also the IM_{Kappos} presents strong correlation with damage measures in SFxy and SWxFy models (Figs. 5a and 5c). This finding is in accordance with the results obtained by Riddell (2007), who concluded that velocity related intensity measures are more effective for the medium-to-long period structures ($T_1 > 0.5s$). Also the $IM_{Mehanny}$ shows strong correlation with the damage measures (MIDR and AIDR) in SWxy and SWxFy models (Figs. 5b and 5c).



(a)

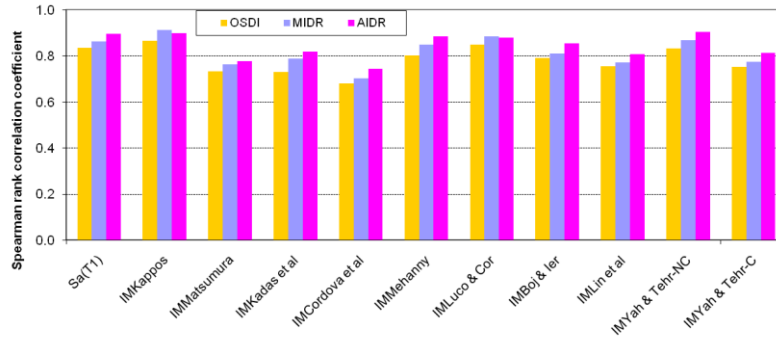


(b)

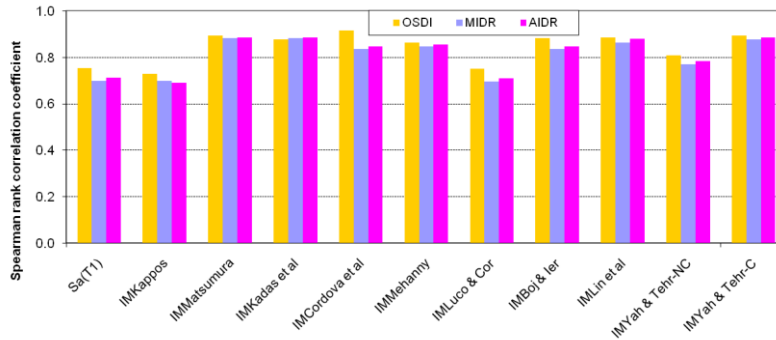


(c)

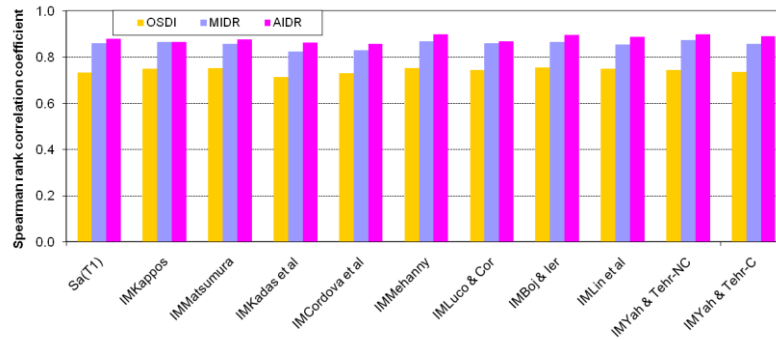
Fig. 5 Spearman rank correlation coefficients between the examined IMs and the three EDPs considered for the double-symmetric buildings (SFxy (a), SWxy (b) and SWxFy (c))



(a)



(b)



(c)

Fig. 6 Spearman rank correlation coefficients between the examined IMs and the three EDPs considered for the asymmetric buildings (AFxy (a), AWxy (b) and AFxWy (c))

The IMs that show strong correlation with the damage measures in the three asymmetric models studied herein are $IM_{Mehanny}$ and $IM_{Boj \& Ier}$ (Fig. 6). In AFxy model the IMs that present strong correlation with the damage measures are: $S_d(T_1)$, IM_{Kappos} , $IM_{Luco \& Cor}$ and $IM_{Yah \& Tehr-NC}$ (Fig. 6(a)). In AWxy model the IMs that present strong correlation with the damage measures are: $IM_{Matsumura}$, $IM_{Kadas \ et \ al.}$, $IM_{Mehanny}$, $IM_{Lin \ et \ al.}$, $IM_{Yah \& Tehr-C}$ and $IM_{Boj \& Ier}$ (Fig. 6b). Finally, in AFxWy model all the examined IMs present strong correlation with the damage measures (MIDR and AIDR).

Another observation is that the damage measure (OSDI, MIDR and OSDI) exhibited stronger correlation with the IM introduced by Mehanny than with the one proposed by Cordova *et al.* (Figs. 5 and 6). The only exception is the building AWxy (Fig. 6b). This was expected since $IM_{Mehanny}$ is an improved version of the $IM_{Cordova\ et\ al.}$. Moreover, comparing the IMs proposed by Yahyaabadi and Tehranizadeh for Non-Collapse and for Collapse seismic demand prediction, it can be seen that the first one leads to larger correlation coefficients. This observation, which is valid for all the buildings except the AWxy, can be explained on the basis of Fig. 4. From this figure it is obvious that the vast majority of the earthquake records used in the present study cause minor or moderate damage to the examined buildings and only a very small number of them lead to severe damage or collapse. Thus the $IM_{Yah\ \&\ Tehr-NC}$ is more appropriate to describe the seismic damage of the structures than the $IM_{Yah\ \&\ Tehr-C}$.

Taking into account all the above results we see that the correlation between the damage measures of the buildings and the structure-specific seismic IMs depends on the EDP, the building features and the IM adopted, hence it is difficult to choose a single IM as the best indicator of structural seismic performance for all the six buildings.

With regard to the building AWxy, we see that the results are in general different from the ones produced for the rest of the buildings. For example, note that the correlation between the IMs proposed by Matsutamura, Kadas *et al.* and Cordova *et al.* is higher than the one produced in case of the other IMs. Moreover, the IMs introduced by Luco and Cornell and by Kappos lead to the smallest correlation coefficients relatively to the other IMs. However, the opposite conclusions have been reached for the other five buildings. The different results obtained for the structural system AWxy may be attributed to the large eccentricity that this building possesses (Fig. 2b).

Of particular importance is also the fact that the widely used spectral acceleration at the fundamental period of the structure is a relatively good predictor of the structural performance, since it shows strong enough correlation with the seismic damage. Note that the correlation coefficients for the five studied models (SFxy, SWxy, SWxFy, AFxy and AFxWy) exhibit values larger than 0.8 when the MIDR or AIDR are considered as damage measures (Figs. 5 and 6). For example the Spearman's correlation coefficient corresponding to $S_a(T_1)$ reaches the value of 0.92 when the MIDR of the building SWxFy is used (Fig. 5c). The relationship between $S_a(T_1)$ and MIDR for this building is shown in Fig. 7, from which it is obvious that the two variables exhibit a

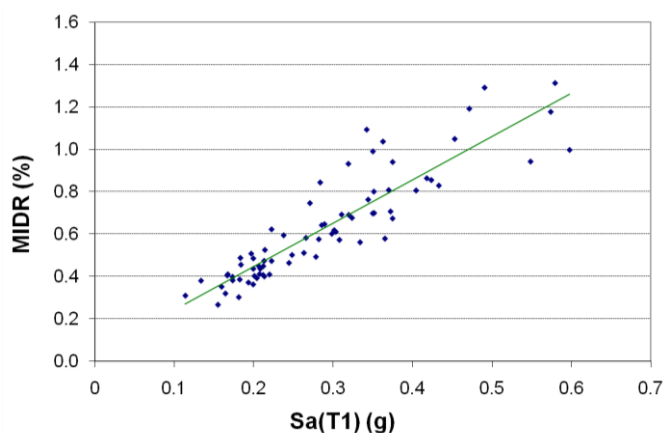


Fig. 7 Relationship between $S_a(T_1)$ and MIDR for the building SWxFy

high degree of correlation between each other. This observation, which is valid for the five of the six structures investigated in the present study (the only exception is the building AW_{xy}), can be attributed to the fact that the performance of the five buildings is dominated by the first two modes of vibration for excitation along x and y axes. The modal participating mass ratios attain values greater than 70% for at least one of the first two mode shapes. Also we see that in these two modes the translational components of vibration dominate. Moreover there is a small degree of coupling between modes (Table 2). On the contrary, concerning the building AW_{xy}, we see that the modal participating mass ratios attain relatively small values for excitation along x and y axes (52% and 59%, respectively, Table 2). Also we can see that the first two modes of vibration have a significant degree of coupling between each other as well as with the modes that the rotational components of vibration dominate. As a consequence, $S_a(T_1)$, which accounts only for the first two modes of vibration for excitation along the x and y axes, cannot adequately capture the high rotational-translational coupling effects.

5. Conclusions

The aim of the present paper is to examine the interdependency between ten advanced, scalar structure-specific ground motion IMs and the seismic damage of earthquake resistant 3D, R/C buildings. To achieve this, six medium-rise R/C buildings with different structural systems are investigated. The buildings are subjected to 74 bidirectional earthquake ground motions for which nonlinear time history analyses are conducted. The evaluation of the expected structural damage state of each building is made by using the Park and Ang Overall Structural Damage Index (OSDI), as well as the Maximum and Average Interstorey Drift Ratio (MIDR and AIDR). The comparative assessment of the results has led to the following conclusions:

- The correlation between the seismic IMs and the structural damage measures that are based on displacements demands (MIDR and AIDR) is stronger than the correlation between IMs and OSDI.

- The IMs proposed by Luco & Cornell, Mehanny, Kappos, as well as by Yahyaabadi and Tehranizadeh for Non-Collapse seismic demand prediction exhibit the highest correlation with the expected damage for most of the buildings. On the other hand, the IMs introduced by Matsumura, Kadas *et al.* and Cordova *et al.* have led to the smallest values of correlation coefficients for the majority of the structures investigated in the present study.

- The widely used spectral acceleration at the fundamental mode period of the structure is a relatively good predictor of the structural performance of all the studied buildings, except the AW_{xy}, that is the building with large structural eccentricity.

It must be noted that the aforementioned conclusions are valid for the buildings and ground motions used in the present study. However, they provide a good insight into the correlation between damage state of 3D, medium rise, R/C buildings under bidirectional excitation and a number of advanced, structure specific IMs. In order to expand them to other structural systems, further investigation is necessary.

Acknowledgments

This study was financially supported by “IKY FELLOWSHIPS OF EXCELLENCE FOR

POSTGRADUATE STUDIES IN GREECE - SIEMENS PROGRAM". The authors would also like to thank Dr. Konstantinos Morfidis for his help in designing the buildings investigated.

References

- ASCE/SEI 41-06 (2008), *Seismic Rehabilitation of Existing Buildings*, American Society of Civil Engineers, Reston, VA.
- Benjamin, J.R. and Cornell, C.A. (1970), *Probability, Statistics and Decision for Civil Engineers*, McGraw Hill, Inc., New York.
- Beyer, K. and Bommer, J. (2006), "Relationships between median values and between aleatory variabilities for different definitions of the horizontal component of motion", *Bull. Seismol. Soc. Am.*, **96**(4A), 1512-1522.
- Bojorquez, E. and Iervolino, I. (2011), "Spectral shape proxies and nonlinear structural response", *Soil Dyn. Earthq. Eng.*, **31**(7), 996-1008.
- Cantagallo, C., Camata, G., Spacone, E. and Corotis, R. (2012), "The variability of deformation demand with ground motion intensity", *Prob. Eng. Mech.*, **28**, 59-65.
- Carr, A. (2004), *Ruaumoko - a Program for Inelastic Time-History Analysis, Program Manual*, Department of Civil Engineering, University of Canterbury, New Zealand.
- Chopra, A.K. (2001), *Dynamics of Structures: Theory and Applications to Earthquake Engineering (2nd edn)*, Prentice-Hall: Englewood Cliffs, NJ.
- Cordova, P.P., Deierlein, G.G., Mehanny, S.S.F. and Cornell, C.A. (2000), "Development of a two-parameter seismic intensity measure and probabilistic assessment procedure", *Proceedings of the 2nd US-Japan Workshop on Performance-Based Earthquake Engineering Methodology for RC Building Structures*, Sapporo, Hokkaido, Japan.
- Cornell, C.A. and Krawinkler, H. (2000), *Progress and Challenges in Seismic Performance Assessment*, PEER Center News.
- Dimova, A.L. and Negro, P. (2005), "Seismic assessment of an industrial frame structure designed according to Eurocodes. Part 2: Capacity and vulnerability", *Eng. Struct.*, **27**(5), 724-735.
- Elenas, A. and Meskouris, K. (2001), "Correlation study between seismic acceleration parameters and damage indices of structure", *Eng. Struct.*, **23**(6), 698-704.
- EC2 (2004), *Design of concrete structures, Part 1-1: General rules and rules for buildings*, European Committee for Standardization, Brussels.
- EC8 (2003), *Design provisions for earthquake resistance of structures*, European Committee for Standardization, Brussels.
- European Strong-Motion Database (2003), http://www.isesd.hi.is/ESD_Local/frameset.htm.
- FEMA 356 (2000), *Prestandard and Commentary for the Seismic Rehabilitation of Buildings*, Federal Emergency Management Agency, Washington, DC.
- Fontara, I.-K.M., Athanatopoulou, A.M. and Avramidis, I.E. (2012), "Correlation between advanced, structure-specific ground motion intensity measures and damage indices", *Proceedings of the 15th World Conference on Earthquake Engineering*, Lisbon, Portugal.
- Giovenale, P., Cornell, C.A. and Esteva, L. (2004), "Comparing the adequacy of alternative ground motion intensity measures for the estimation of structural responses", *Earthq. Eng. Struct. Dyn.*, **33**(8), 951-979.
- Gunturi, S.K.V. and Shah, H.C. (1992), "Building specific damage estimation", *Proceedings of 10th World Conference on Earthquake Engineering*, Madrid, Spain. Balkema, Rotterdam.
- Imbsen Software Systems (2006), *XTRACT: Version 3.0.5. Cross-Sectional Structural Analysis of Component, Program Manual*, Sacramento, CA.
- Kadas, K., Yakut, A. and Kazaz, I. (2011), "Spectral ground motion intensity based on capacity and period elongation", *J. Struct. Eng.*, ASCE, **137**(3), 401-409.
- Kappos, A.J. (1990), "Sensitivity of calculated inelastic seismic response to input motion characteristics",

- Proceedings of 4th National Conference on Earthquake Engineering*, Palm Springs, California, USA.
- Kostinakis, K., Papadopoulos, M. and Athanatopoulou, A. (2014), "Adequacy of advanced earthquake intensity measures for estimation of damage under seismic excitation with arbitrary orientation", *Proceedings of International Conference on Civil, Structural and Earthquake Engineering*, Paris, France.
- Kostinakis, K., Athanatopoulou, A. and Morfidis, K. (2015), "Correlation between ground motion intensity measures and seismic damage of 3D R/C buildings", *Eng. Struct.*, **82**, 151-167.
- Kunnath, S.K., Reinhorn, A.M. and Lobo, R.F. (1992), *IDARC Version 3: A Program for the Inelastic Damage Analysis of R/C Structures*, Technical Report NCEER-92-0022, National Centre for Earthquake Engineering Research, State University of New York, Buffalo, NY.
- Lin, L. (2008), "Development of improved intensity measures for probabilistic seismic demand analysis" Ph.D. Thesis, Department of Civil Engineering, University of Ottawa, Ottawa, Ont., Canada.
- Lin, L., Naumoski, N., Saatcioglu, M. and Foo, S. (2011), "Improved intensity measures for probabilistic seismic demand analysis, Part 1: development of improved intensity measures", *Can. J. Civ. Eng.*, **38**(1), 79-88.
- Luco, N. (2002), "Probabilistic seismic demand analysis, SMRF connection fractures, and near-source effects", Ph.D. Thesis, Department of Civil and Environmental Engineering, Stanford University, CA.
- Luco, N. and Cornell, C.A. (2007), "Structure-specific scalar intensity measures for near-source and ordinary earthquake motions", *Earthq. Spectra*, **23**(2), 357-392.
- Masi, A., Vona, M. and Mucciarelli, M. (2011), "Selection of natural and synthetic accelerograms for seismic vulnerability studies on reinforced concrete frames", *J. Struct. Eng.*, **137**(3), 367-378.
- Matsumura, K. (1992), "On the intensity measure of strong motion related to structural failures", *Proceedings of 10th World Conference on Earthquake Engineering*, Rotterdam, Netherlands.
- Mehanny, S.S.F. (2009), "A broad-range power-law form scalar-based seismic intensity measure", *Eng. Struct.*, **31**(7), 1354-1368.
- Mori, Y., Yamanaka, T., Luco, N., Nakashima, M. and Cornell, C.A. (2004), "Predictors of seismic demand of SMRF buildings considering post-elastic mode shape", *Proceedings of the 13th World Conference on Earthquake Engineering*, Vancouver, Canada.
- Naeim, F. (2001), *The Seismic Design Handbook*, Kluwer Academic, Boston.
- NEHRP (2003), *Recommended provisions for seismic regulations for new buildings and other Structures*, FEMA450, Building Seismic Safety Council, Washington, DC.
- Otani, A. (1974), "Inelastic analysis of RC frame structures", *J. Struct. Div.*, ASCE, **100**(7), 1433-1449.
- Pacific Earthquake Engineering Research Centre (PEER) (2003), Strong Motion Database. <http://peer.berkeley.edu/smcat/>
- Park, Y.J. and Ang, A.H.-S. (1985), "Mechanistic seismic damage model for reinforced-concrete", *J. Struct. Eng.*, ASCE, **111**(4), 722-739.
- Park, Y.J., Ang, A.H.-S. and Wen, Y.K. (1987), "Damage-limiting aseismic design of buildings", *Earthq. Spectra*, **3**(1), 1-26.
- Penzien, J. and Watabe, M. (1975), "Characteristics of 3-D earthquake ground motions", *Earthq. Eng. Struct. Dyn.*, **3**(4), 365-373.
- RA.F. (2012), *Structural Analysis and Design Software v.3.3.2, Program ManualTOL*, Engineering Software House, Iraklion, Crete, Greece.
- Riddell, R. (2007), "On ground motion intensity indices", *Earthq. Spectra*, **23**(1), 147-173.
- Tothong, P. and Luco, N. (2007), "Probabilistic seismic demand analysis using advanced ground motion intensity measures", *Earthq. Eng. Struct. Dyn.*, **36**(13), 1837-1860.
- Tothong, P. and Cornell, C.A. (2008), "Structural performance assessment under near-source pulse-like ground motions using advanced ground motion intensity measures", *Earthq. Eng. Struct. Dyn.*, **37**(7), 1013-1037.
- UBC Vol. 2 (1997), *Structural Engineering Design Provisions*, International Conference of Building Officials (ICBO), Whittier, CA.
- Yahyaabadi, A. and Tehranizadeh, M. (2011), "New scalar intensity measure for near-fault ground motions based on the optimal combination of spectral response", *Scientia Iranica*, **18**(6), 1149-1158.

Yakut, A. and Yilmaz, H. (2008), "Correlation of deformation demands with ground motion intensity", *J. Struct. Eng.*, **134**(12), 1818-1828.

SA

Appendix

Table A.1 Ground motions recorded on Soil Type C according to EC8

| No | Date | Earthquake name | Magnitude (Ms) | Station name | Closest distance (km) | Component (deg) | PGA (g) | Corr. Factor ρ |
|----|------------|------------------|----------------|-----------------------------|-----------------------|-----------------|----------------|---------------------|
| 1 | 15/10/1979 | Imperial Valley | 6.9 | Chihuahua | 28.7 | 012 282 | 0.270 0.254 | -18.63 |
| 2 | 15/10/1979 | Imperial Valley | 6.9 | Coachella Canal #4 | 49.3 | 045 135 | 0.115 0.128 | 53.33 |
| 3 | 17/08/1999 | Kocaeli, Turkey | 7.8 | Atakoy | 67.5 | 000 090 | 0.105 0.164 | -4.25 |
| 4 | 17/08/1999 | Kocaeli, Turkey | 7.8 | Cekmece | 76.1 | 000 090 | 0.179 0.133 | 12.25 |
| 5 | 28/06/1992 | Landers | 7.4 | Coachella Canal | 55.7 | 000 090 | 0.104 0.109 | 18.52 |
| 6 | 18/10/1989 | Loma Prieta | 7.1 | Halls Valley | 31.6 | 090 180 | 0.134 0.103 | 3.61 |
| 7 | 18/10/1989 | Loma Prieta | 7.1 | Agnews State Hospital | 28.2 | 090 180 | 0.172 0.159 | 15.29 |
| 8 | 18/10/1989 | Loma Prieta | 7.1 | Gilroy Array #7 | 24.2 | 090 180 | 0.226 0.323 | -30.08 |
| 9 | 24/04/1984 | Morgan Hill | 6.1 | Hollister City Hall | 32.5 | 001 271 | 0.071 0.071 | -15.34 |
| 10 | 17/01/1994 | Northridge | 6.7 | Glendale - Las Palmas | 25.4 | 177 267 | 0.357 0.206 | -4.80 |
| 11 | 17/01/1994 | Northridge | 6.7 | LA - Saturn St | 30 | 020 110 | 0.474 0.439 | -6.36 |
| 12 | 02/05/1983 | Coalinga | 6.5 | Parkfield - Cholame 5W | 47.3 | 270 360 | 0.147 0.131 | -9.62 |
| 13 | 02/05/1983 | Coalinga | 6.5 | Parkfield - Cholame 8W | 50.7 | 000 270 | 0.098 0.100 | -27.60 |
| 14 | 17/01/1994 | Northridge | 6.7 | Sun Valley - Roscoe Blvd | 12.3 | 000 090 | 0.303 0.443 | -3.28 |
| 15 | 01/10/1987 | Whittier Narrows | 5.7 | Bell Gardens - Jaboneria | 9.8 | 207 297 | 0.219 0.212 | -2.13 |
| 16 | 01/10/1987 | Whittier Narrows | 5.7 | El Monte - Fairview Av | 9.8 | 000 270 | 0.120 0.228 | 22.70 |
| 17 | 01/10/1987 | Whittier Narrows | 5.7 | Santa Fe Springs - E Joslin | 10.8 | 048 318 | 0.426 0.443 | -8.09 |
| 18 | 19/05/1940 | Imperial Valley | 7.2 | El Centro Array #9 | 8.3 | 180 270 | 0.313 0.215 | -13.03 |

Table A.1 Continued

| No | Date | Earthquake name | Magnitude (Ms) | Station name | Closest distance (km) | Component (deg) | PGA (g) | Corr. Factor ρ |
|--------------|------|-----------------------|----------------|-------------------------------------|-----------------------|-----------------|----------------|---------------------|
| 1928/06/1966 | | Parkfield | | Cholame #5 | 5.3 | 085 355 | 0.442 0.367 | -15.36 |
| 2020/09/1999 | | Chi-Chi, Taiwan | 7.6 | TCU | 2.94 | N W | 0.251 0.202 | -32.97 |
| 2120/09/1999 | | Chi-Chi, Taiwan | 7.6 | TCU | 4.01 | N W | 0.162 0.134 | -10.49 |
| 2220/09/1999 | | Chi-Chi, Taiwan | 7.6 | TCU | 4.5 | N W | 0.251 0.293 | -8.25 |
| 2320/09/1999 | | Chi-Chi, Taiwan | 7.6 | TCU | 10.33 | N W | 0.130 0.147 | -15.17 |
| 2420/09/1999 | | Chi-Chi, Taiwan | 7.6 | TCU | 5.92 | N W | 0.188 0.148 | -25.55 |
| 2518/10/1989 | | Loma Prieta | 7.1 | Gilroy Array #2 | 12.7 | 000 090 | 0.367 0.322 | 26.38 |
| 2618/10/1989 | | Loma Prieta | 7.1 | Gilroy Array #3 | 14.4 | 000 090 | 0.555 0.367 | 4.51 |
| 2718/10/1989 | | Loma Prieta | 7.1 | Capitola | 14.5 | 000 090 | 0.529 0.443 | -22.57 |
| 2801/10/1987 | | Whittier Narrows | 5.7 | LA - Fletcher Dr | 14.4 | 144 234 | 0.171 0.231 | -4.19 |
| 2907/12/1988 | | Spitak | 6.7 | Gukasian | 20 | E-W N-S | 0.183 0.183 | -4.54 |
| 3020/06/1990 | | Manjil (Iran) | 7.4 | Abhar | 75 | N57E N33W | 0.132 0.209 | -33.38 |
| 3117/08/1999 | | Izmit (Turkey) | 7.6 | Izmit-Karayollari Sefligi Muracaati | 29 | W-E S-N | 0.129 0.091 | 1.75 |
| 3217/08/1999 | | Izmit (Turkey) | 7.6 | Istanbul-Zeytinburnu | 80 | E-W N-S | 0.114 0.110 | 5.34 |
| 3311/09/1976 | | Friuli (Italy) | 5.5 | Buia | 7 | E-W N-S | 0.105 0.230 | 3.80 |
| 3415/09/1976 | | Friuli (Italy) | 6 | Buia | 9 | E-W N-S | 0.095 0.109 | -6.81 |
| 3524/02/1981 | | Aktion (Greece) | 6.6 | Korinthos-OTE Building | 10 | N30 N120 | 0.230 0.310 | -28.07 |
| 3626/09/1997 | | Umbria Marche (Italy) | 6 | Colfiorito | 5 | N-S W-E | 0.199 0.223 | -10.76 |
| 3717/08/1999 | | Izmit Turkey) | 7.6 | Yarimca-Petkim | 5 | E-W N-S | 0.244 0.296 | 6.07 |

Table A.1 Continued

| No | Date | Earthquake name | Magnitude (Ms) | Station name | Closest distance (km) | Component (deg) | PGA (g) | Corr. Factor ρ |
|----|------------|------------------|----------------|-----------------------------|-----------------------|-----------------|----------------|---------------------|
| 38 | 12/11/1999 | Duzce Turkey) | 7.2 | LDEO Station No. C1062 FI | 14 | E-W N-S | 0.254 0.114 | 12.82 |
| 39 | 15/10/1979 | Imperial Valley | 6.9 | Delta | 43.6 | 262 352 | 0.238 0.351 | 5.92 |
| 40 | 28/06/1992 | Landers | 7.4 | Yermo Fire Station | 24.9 | 270 360 | 0.245 0.152 | -19.97 |
| 41 | 27/01/1980 | Livermore | 5.5 | San Ramon - Eastman Kodak | 17.6 | 180 270 | 0.301 0.097 | -23.09 |
| 42 | 18/10/1989 | Loma Prieta | 7.1 | Gilroy Array #4 | 16.1 | 000 090 | 0.417 0.212 | 5.98 |
| 43 | 18/10/1989 | Loma Prieta | 7.1 | SF Intern. Airport | 64.4 | 000 090 | 0.236 0.329 | 19.31 |
| 44 | 18/10/1989 | Loma Prieta | 7.1 | Oakland - Title & Trust | 77.4 | 180 270 | 0.195 0.244 | 2.85 |
| 45 | 18/10/1989 | Loma Prieta | 7.1 | Sunnyvale - Colton Ave. | 28.2 | 270 360 | 0.207 0.209 | -9.66 |
| 46 | 17/01/1994 | Northridge | 6.7 | LA - Centinela St | 30.9 | 155 245 | 0.465 0.322 | -10.16 |
| 47 | 17/01/1994 | Northridge | 6.7 | LA - Fletcher Dr | 29.5 | 144 234 | 0.162 0.240 | 16.52 |
| 48 | 17/01/1994 | Northridge | 6.7 | LA - N Faring Rd | 23.9 | 000 090 | 0.273 0.242 | -17.96 |
| 49 | 17/01/1994 | Northridge | 6.7 | LA - S Grand Ave | 36.9 | 090 180 | 0.290 0.264 | -6.95 |
| 50 | 17/01/1994 | Northridge | 6.7 | Manhattan Beach - Manhattan | 42 | 000 090 | 0.201 0.128 | 7.18 |
| 51 | 17/01/1994 | Northridge | 6.7 | Point Mugu - Laguna Peak | 47.6 | 000 090 | 0.134 0.223 | 2.76 |
| 52 | 09/02/1971 | San Fernando | 6.6 | LA - Hollywood Stor Lot | 21.2 | 090 180 | 0.210 0.174 | 18.12 |
| 53 | 24/11/1987 | Superstitt Hills | 6.6 | Calipatria Fire Station | 28.3 | 225 315 | 0.180 0.247 | 16.67 |
| 54 | 01/10/1987 | Whittier Narrows | 5.7 | Compton - Castlegate St | 16.9 | 000 270 | 0.332 0.333 | -36.20 |
| 55 | 01/10/1987 | Whittier Narrows | 5.7 | Downey - Birchdale | 56.8 | 090 180 | 0.243 0.299 | -6.38 |
| 56 | 01/10/1987 | Whittier Narrows | 5.7 | Downey - Co Maint Bldg | 18.3 | 180 270 | 0.221 0.141 | 45.73 |

Table A.1 Continued

| No | Date | Earthquake name | Magnitude (Ms) | Station name | Closest distance (km) | Component (deg) | PGA (g) | Corr. Factor ρ |
|--------------|------|------------------|----------------|-----------------------------|-----------------------|-----------------|----------------|---------------------|
| 5701/10/1987 | | Whittier Narrows | 5.7 | Glendale - Las Palmas | 19 | 177 267 | 0.296 0.166 | 3.90 |
| 5801/10/1987 | | Whittier Narrows | 5.7 | Lakewood - Del Amo Blvd | 20.9 | 000 090 | 0.277 0.178 | 15.08 |
| 5901/10/1987 | | Whittier Narrows | 5.7 | Studio City - Coldwater Can | 28.7 | 092 182 | 0.177 0.231 | -11.36 |
| 6008/07/1986 | | N. Palm Springs | 6 | Palm Springs Airport | 16.6 | 000 090 | 0.158 0.187 | 13.83 |
| 6117/01/1994 | | Northridge | 6.7 | LA - Pico & Sentous | 32.7 | 090 180 | 0.103 0.186 | -4.68 |
| 6217/01/1994 | | Northridge | 6.7 | Leona Valley #6 | 38.5 | 090 360 | 0.178 0.131 | -1.67 |
| 6324/11/1987 | | Superstitt Hills | 6.6 | Plaster City | 21 | 045 135 | 0.121 0.186 | 27.34 |
| 6424/01/1980 | | Livermore | 5.5 | San Ramon - Eastman Kodak | 17.6 | 180 270 | 0.154 0.076 | -34.55 |
| 6518/10/1989 | | Loma Prieta | 7.1 | APEEL 2E Hayward Muir Sch | 57.4 | 000 090 | 0.171 0.139 | -3.69 |
| 6615/10/1979 | | Imperial Valley | 6.9 | Aeropuerto Mexicali | 8.5 | 045 315 | 0.327 0.260 | -6.94 |
| 6715/10/1979 | | Imperial Valley | 6.9 | Calexico Fire Station | 10.6 | 225 315 | 0.275 0.202 | 4.09 |
| 6815/10/1979 | | Imperial Valley | 6.9 | EC County Center FF | 7.6 | 002 092 | 0.213 0.235 | -19.05 |
| 6915/10/1979 | | Imperial Valley | 6.9 | El Centro Array #6 | 1 | 140 230 | 0.41 0.439 | -12.22 |
| 7015/10/1979 | | Imperial Valley | 6.9 | El Centro Array #10 | 8.6 | 050 320 | 0.171 0.224 | 13.42 |
| 7115/10/1979 | | Imperial Valley | 6.9 | Holtville Post Office | 7.5 | 225 315 | 0.253 0.221 | 1.88 |
| 7224/11/1987 | | Superstitt Hills | 6.6 | El Centro Imp. Co. Cent | 13.9 | 000 090 | 0.358 0.258 | 9.45 |
| 7324/11/1987 | | Superstitt Hills | 6.6 | Westmorland Fire Sta | 13.3 | 090 180 | 0.172 0.211 | 8.15 |
| 7424/04/1984 | | Morgan Hill | 6.1 | Gilroy Array #4 | 12.8 | 270 360 | 0.224 0.348 | -36.09 |